Journal Pre-proof

Electrochemical simulation of metabolic reduction and conjugation reactions of unsymmetrical bisacridine antitumor agents, C-2028 and C-2053

Agnieszka Potęga (Conceptualization) (Methodology) (Validation) (Formal analysis)<ce:contributor-role>Writing - original draft, Writing - review and editing) (Visualization), Szymon Paczkowski (Validation) (Formal analysis) (Writing - original draft), Ewa Paluszkiewicz (Formal analysis), Zofia Mazerska (Writing - original draft)

Please cite this article as: Potęga A, Paczkowski S, Paluszkiewicz E, Mazerska Z, Electrochemical simulation of metabolic reduction and conjugation reactions of unsymmetrical bisacridine antitumor agents, C-2028 and C-2053, *Journal of Pharmaceutical and Biomedical Analysis* (2021), doi: https://doi.org/10.1016/j.jpba.2021.113970

This is a PDF file of an article that has undergone enhancements after acceptance, such as the addition of a cover page and metadata, and formatting for readability, but it is not yet the definitive version of record. This version will undergo additional copyediting, typesetting and review before it is published in its final form, but we are providing this version to give early visibility of the article. Please note that, during the production process, errors may be discovered which could affect the content, and all legal disclaimers that apply to the journal pertain.

© 2020 Published by Elsevier.

Title page

Title:

Electrochemical simulation of metabolic reduction and conjugation reactions of unsymmetrical bisacridine antitumor agents, C-2028 and C-2053.

Authors:

Agnieszka Potęga, Szymon Paczkowski, Ewa Paluszkiewicz, Zofia Mazerska

Affiliations:

Department of Pharmaceutical Technology and Biochemistry, Faculty of Chemistry, Gdańsk University of Technology, Gabriela Narutowicza St. 11/12, Gdańsk 80-233, Poland.

agnieszka.potega@pg.edu.pl (A.P.), szymon.paczkowski@aol.com (Sz.P.), ewa.paluszkiewicz@pg.edu.pl (E.P.), zofia.mazerska@pg.edu.pl (Z.M.)

Corresponding author:

Agnieszka Potęga

Department of Pharmaceutical Technology and Biochemistry, Faculty of Chemistry, Gdańsk University of Technology, Gabriela Narutowicza St. 11/12, Gdańsk 80-233, Poland.

e-mail: agnieszka.potega@pg.edu.pl, telephone: +48 58 347 15 93, fax: +48 58 347 11 44

Research highlights

- Reductive metabolism of potent antitumor agents was simulated by electrochemistry.

- Electrochemistry allowed to produce reactive nitroso and hydroxylamine species.

- *N*-oxide of antitumor bisacridine was found as a prodrug under hypoxic conditions.

- Reactive products were studied in respect to their interaction with biomolecules.

- GSH and DTT adducts were observed after reductive metabolism of antitumor C-2028.

Abstract

Electrochemistry (EC) coupled with analysis techniques such as liquid chromatography (LC) and mass spectrometry (MS) has been developed as a powerful tool for drug metabolism simulation. The application of EC in metabolic studies is particularly favourable due to the low matrix contribution compared to *in vitro* or *in vivo* biological models. In this paper, the EC(/LC)/MS system was applied to simulate phase I metabolism of the representative two unsymmetrical bisacridines (UAs), named C-2028 and C-2053, which contain nitroaromatic group susceptible to reductive transformations. UAs are a novel potent class of antitumor agents of extraordinary structures that may be useful in the treatment of difficult for therapy human solid tumors such as breast, colon, prostate, and pancreatic tumors. It is considered that the biological action of these compounds may be due to the redox properties of the nitroaromatic group. At first, the relevant conditions for the electrochemical conversion and product identification process, including the electrode potential range, electrolyte composition, and working electrode material, were optimized with the application of 1-nitroacridine as a model compound. Electrochemical simulation of C-2028 and C-2053 reductive metabolism resulted in the generation of six and five products, respectively. The formation of hydroxylamine m/z [M+H-14]$^+$, amine m/z [M+H-30]$^+$, and novel *N*-oxide m/z [M+H-18]$^+$ species from UAs was demonstrated. Furthermore, both studied compounds were shown to be stable, retaining their dimeric forms, during electrochemical experiments. The electrochemical method also indicated the susceptibility of C-2028 to phase II metabolic reactions. The respective glutathione and dithiothreitol adducts of C-2028 were identified as ions at m/z 873 and m/z 720. In conclusion, the electrochemical reductive transformations of antitumor UAs allowed for the synthesis of new reactive intermediate forms permitting the study of their interactions with biologically crucial molecules.

Abbreviations

ACN, acetonitrile; C-2028, 9-{*N*-[(imidazo[4,5,1-de]-acridin-6-on-5-yl)aminopropyl]-*N*-methylaminopropylamino}-1'-nitroacridine; C-2053, 9-{*N*-[(imidazo[4,5,1-de]-acridin-6-on-5-yl)aminopropyl]-*N*-methylaminopropylamino}-4'-methyl-1'-nitroacridine; BDD, boron-doped diamond; DTT, dithiothreitol; EC, electrochemistry, electrochemical; ESI, electrospray ionization; FA, formic acid; GC, glassy carbon; GSH, L-glutathione reduced; LC, liquid chromatography; MeOH, methanol; *m/z*, mass-to-charge ratio; MS, mass spectrometry, mass spectrometer; MS/MS, tandem mass spectrometry; P450, cytochrome P450; Q-TOF, quadrupole-time of flight; UA, unsymmetrical bisacridine;

1. Introduction

The development of a new drug requires careful consideration of its metabolism and elimination after administration into the human organism [1]. During *in vivo* metabolism reactions the parent drug is usually enzymatically converted to metabolites of higher polarity and better solubility in water (phase I metabolism), what improves its excretion outside the body [2]. Although metabolism aims to inactivate xenobiotics, some drug metabolites may be pharmacologically active – sometimes even more in comparison to the original compound. Furthermore, certain metabolic reactions in the cell might lead to the generation of reactive intermediates, what may be implicated in the toxicity as a result of their covalent binding to biomolecules [3]. Therefore, early knowledge about pharmacological and/or toxicological effects of drug metabolites is extremely desired for assessing its bioavailability, activity, and safety profiles in humans.

The most important enzyme system of phase I metabolism is cytochrome P450 (P450), a microsomal superfamily of isoenzymes, which catalyzes oxidation, reduction, or hydrolysis of many drugs [4]. In order to predict such metabolic pathways, a few *in vivo* (*e.g.*, with mice or rats) and *in vitro* (*e.g.*, by incubation with hepatocytes or liver microsomes) procedures have been developed [5,6]. However, these strategies are relatively complex, expensive, and time-

consuming. Thus, other investigative methods, the alternative to those on biological materials, have been established to predict drug metabolism [7]. Among them, electrochemistry coupled on-line with mass-spectrometry (EC/MS) is of significant interest [8]. This non-enzymatic technique has shown very promising results in the generation of a variety of metabolites, including reactive metabolites. These are formed with relatively high concentrations in a matrix-free electrochemical environment what allows for extensive model studies on drug metabolism and/or toxicology [8,9].

The development of the EC/MS technique for the efficient simulation of P450-mediated oxidation reactions has been reviewed by several authors [10-12]. However, P450 enzymes also express the ability to produce metabolites through a reduction mechanism [4]. Specifically, the nitroaromatic compounds of biological significance represent the type of agents, biological functions of which (pharmacological or toxicological) result probably from the redox properties of the nitroaromatic functional group [13]. The general multistep pathway of the reductive transformation of the nitroaromatic compound to its corresponding amine derivative was shown in Fig. 1 [14]. Due to highly reactive nature, the resulted nitro radical anion, nitroxyl radical, nitroso, and hydroxylamine species can bind covalently to biomolecules causing possibly toxic reactions [15]. On the other hand, their conjugation (phase II metabolism) with nucleophiles such as reduced glutathione (GSH) might be the organism's defense against toxicity [16]. So far, the mechanisms of electrochemical reduction of nitroaromatic compounds have been shown to be very complex and strongly dependent on the reaction medium [13]. In fact, these studies have been usually limited to the determination of nitro radical anion which is the first intermediate product in the reduction pathway of nitro compounds. Therefore, increasing attention is being paid to the potential of the EC/MS technique for the generation and identification of other reduced species. Further, characterization of the adducts of reactive intermediates with small molecule trapping agents can indicate the structure of primary reactive species from which they are derived. Thereby, these studies allow understanding the molecular mechanisms of bioactivation pathways.

4

Continuing the search for antitumor drug candidates, a completely novel class of acridine derivatives, unsymmetrical bisacridines (UAs) [17,18], has been synthesized and developed by our research group. The compounds were active not only against a set of tumor cell lines but also against human tumor xenografts in nude mice. The promising results from these initial studies give hope for the application of UAs in the treatment or the prevention of tumors that are usually resistant to therapy. Although dimeric compounds with pharmacological properties are known from the state of the art, UAs are distinguished from other acridine dimers by an extraordinary structure. These are combinations (by using an appropriate linker) of monomeric imidazoacridinones and 1-nitroacridines (Fig. 2A), which antitumor activity and metabolic transformations have been previously demonstrated [19-21]. However, the crucial assumption for the synthesis of new dimeric compounds was the high antitumor activity of UAs resulted from the characteristic feature of the unsymmetrical dimeric structure, not from the sum of the monomer activities. The preliminary results of studies on UA metabolism clearly indicated that the main transformation pathway of these compounds is the specific reduction of the nitro group by P450 isoenzymes (unpublished data). Thus, it is supposed to be one of the activation steps leading to covalent binding of the drug to biomacromolecules both in subcellular systems and in the cell.

Considering all the above, the aim of the present study was to investigate metabolic reduction and conjugation reactions of the representative two UAs, named C-2028 and C-2053 (Fig. 2A), by the way of the electrochemical simulation method. In this work, 1-nitroacridine molecule (Fig. 2B) was selected as a model compound for the evaluation of electrochemical conditions for the reduction of the nitroaromatic moiety. The products of UAs transformations, generated in an electrochemical cell, were identified by mass spectrometry. Then, the results obtained from EC/MS analyses were correlated with the results from previous enzymatic experiments. The possibility to simulate the binding of reactive metabolites to small molecule trapping agents (*i.e.*, reduced GSH, dithiothreitol) will be also discussed. Moreover, we assessed the effect of the methyl (electron-donating) substituent on the nitroacridine moiety on the susceptibility of the investigated compounds to reductive transformations, what may

5

affect the final action of a potential drug. The proposed studies will extend the knowledge about the molecular mechanism of metabolic transformations of the investigated UAs. Our findings will also allow to predict the optimal strategy for achieving a balance between antitumor therapeutic efficacy and toxic effects of these potent chemotherapeutics.

2. Materials and methods

2.1. Chemicals

Unsymmetrical bisacridines, 9-{N-[(imidazo[4,5,1-de]-acridin-6-on-5-yl)aminopropyl]-N-methylaminopropylamino}-1'-nitroacridine (C-2028) and 9-{N-[(imidazo[4,5,1-de]-acridin-6-on-5-yl)aminopropyl]-N-methylaminopropylamino}-4'-methyl-1'-nitroacridine (C-2053) (Fig. 2A), and 1-nitroacridine model compound (Fig. 2B) were synthesized and purified in our laboratory according to the method described earlier [17,18,22]. Dithiothreitol (DTT), formic acid (FA), and L-glutathione reduced (GSH) were purchased from Sigma-Aldrich (St. Louis, MO, USA) while ammonium formate (NH_4HCO_2) was ordered from Fisher Scientific (Loughborough, UK). Methanol (MeOH) and acetonitrile (ACN) (both in gradient grade quality for liquid chromatography) were obtained from Merck KGaA (Darmstadt, Germany). Ultrapure water (conductivity 0.056 μS cm^{-1}), used in all the experiments, was passed through a Milli-Q water purification system from Merck KGaA.

2.2. General instrumentation

The experiments were performed using two analysis techniques: (i) direct (on-line) connection of electrochemical cell with electrospray ionization mass spectrometry (EC/ESI-MS) and (ii) off-line connection of electrochemistry with liquid chromatography to electrospray ionization mass spectrometry (EC LC/ESI-MS). Tandem mass spectrometry (MS/MS) mode was used to provide additional structural information for the ions of interest.

2.2.1. Electrochemistry/mass spectrometry (EC/MS)

The EC system used for electrochemical simulation of P450-mediated redox reactions was set up as reported in previous investigations [23,24]. It contained a commercial electrochemical thin-layer ReactorCell™ supplied to a disc glassy carbon (GC) or boron-doped diamond (BDD) working electrode (ϕ = 8 mm; A = 0.502 cm^2), the HyREF™ palladium-hydrogen (Pd/H$_2$)

6

reference electrode, and an upper part of the inlet block made of the carbon-loaded polytetrafluoroethylene as auxiliary electrode (a three-electrode configuration) from Antec Leyden (Zoeterwoude, The Netherlands). In the case of loss of sensitivity due to fouling or compound absorption, the surface of GC working electrode was wiping with a tissue wetted with MeOH and/or was finished with a polishing disc and diamond slurry provided by the manufacturer (Antec Leyden) prior to each experiment. The BDD working electrode consisted of an ultra-thin crystalline diamond layer deposited on top of a silicon substrate. Therefore, its surface was restored not by polishing but electrochemically using pulse mode under acidic conditions. Electrochemical measurements were carried out via the ROXY™ potentiostat driven by Dialogue software from Antec Leyden. The sample solutions for electrochemical analysis were infused through the EC system using a SP2-ROXY™ Dual-Piston Syringe Pump (Antec Leyden). For LC/ESI-MS and/or LC/Q-TOF-MS/MS analyses, electrochemical mixtures were collected in vials and stored at -20ºC until analysis.

Coupling of EC/MS was achieved by the connection of the outlet of the EC cell to the ESI source of a guadrupole mass spectrometer LCMS-2020 (Shimadzu Corp., Kyoto, Japan) inlet using 50 cm long PEEK tubing (130 µm I.D.). For controlling the MS LabSolutions software (Shimadzu Corp.) was used. ESI-MS detection of products generated by EC was performed out in the positive ion mode (+) in the full scan mode (mass-to-charge ratio, *m/z* 100-1500). The detailed ESI-MS parameters were presented in Table 1.

2.2.2. Liquid chromatography/mass spectrometry (LC/MS)

Liquid chromatography/mass spectrometry (LC/MS) experiments were carried out on a Nexera-I LC-2040C 3D high-performance LC system coupled with the LCMS-2020 system through an ESI interface (Shimadzu Corp.). 50 µL of mixture obtained after electrochemical analysis was separated on a reversed-phase 5-µm Suplex pKb-100 analytical column (C18) (Supelco Inc., Bellefonte, PA, USA) with the following dimensions: 250 mm length x 4.6 mm i.d., 5-µm particle size, at a room temperature. A gradient at 0.8 mL min^{-1}, between solvents A, 0.05 M aqueous NH_4HCO_2 buffer (pH 3.4 adjusted with FA), and B, MeOH, was used for chromatographic separation. A linear gradient from 15% to 85% B in A was kept for 25 minutes,

then followed by a linear gradient from 80% to 100% B in A for 3 minutes. A rate of 100% of solvent B was kept for 1.5 min before returning to initial conditions within 0.5 min. These were then kept for 10 min to allow for column equilibration. The eluates were monitored with UV-vis detection and/or diode array and multiple wavelength detection. The ESI-MS conditions were identical to those presented above.

LC/MS/MS analyses were performed with an Agilent 6500 Series Accurate-Mass Quadrupole-Time of Flight (Q-TOF) mass spectrometer (Agilent Technologies, Santa Clara, CA, USA) controlled by Agilent MassHunter Workstation software. To ensure accurate mass during the experiment, the mass spectrometer was calibrated daily using calibration solution (ES-TOF reference mix, Agilent Technologies). The optimized parameters for the ESI-ion trap MS/MS experiments can be viewed in Table 1.

2.3. Electrochemical simulation of the reductive metabolism of UAs

1-Nitroacridine and the investigated UAs were separately dissolved in an electrolyte solution to reach the concentration of 10 μM. Two electrolytes of different composition were used for optimization of the electrochemical conditions: (1) H_2O-MeOH (1:1, *v/v*) with 0.1% FA,; (2) 20 mM NH_4HCO_2-ACN (1:1, *v/v*), pH~3.3 (adjusted to appropriate pH by FA). Simulation of the reduction reactions of the compounds in the EC cell was accomplished at a constant flow rate of 20 μL min^{-1}. The working potential was swept from -2500 to -500 mV with incremental steps of 5 mV s^{-1} and was controlled by the Dialogue software (Antec Leyden). The outlet of the EC cell was connected on-line to the ESI-MS source. To register mass intensity-potential curves the continuous scan mode was used. Representative results of at least three independent experiments were considered.

Stock solutions of reduced GSH and DTT were prepared in ultrapure water at a concentration of 100 mM shortly before each experiment. For the formation of GSH or DTT adducts with reactive products of UAs electrochemical conversion, GSH or DTT were added directly to the mixture obtained from electrochemical analysis (post-electrochemical mixture) to reach the final concentration of 5 mM. Samples exposed to DTT were additionally incubated

8

in a water bath for 30 min incubation at 37ºC. The incubation mixtures were then analysed by LC/MS/MS.

3. Results and discussion

3.1. Optimization of experimental electrosynthesis conditions

The products of drug metabolism that express high chemical reactivity are usually difficult to detect and identify in complex biological matrices. In order to generate them in a matrix-free environment with relatively high amounts, EC analysis coupled with MS detection can be performed. In this work, the optimization of the EC method for the effective synthesis (electrosynthesis) of both stable and reactive reduction products of nitroaromatic compounds was accomplished using 1-nitroacridine as a model structure. In this experiment the influence of the following parameters on the efficiency of the electrochemical conversion was investigated:

- type of electrolyte: aqueous formic acid (FA) solution, ammonium formate (NH_4HCO_2);
- working electrode material: glassy carbon (GC), boron-doped diamond (BDD).

The electrochemical reduction of the aromatic nitro group towards the formation of three major species: nitroso, hydroxylamine, and amine (Fig. 1) requires an aqueous (protic) medium and is favoured in acidic solution [14,25]. Under these conditions, the nitro radical anion produced by a single-electron transfer in the first stage of the process quickly undergoes a protonation, which allows for the subsequent reactions. Two acidic electrolytes (pH~3.3) were used in combination with various working electrode materials in order to obtain a comprehensive overview of the formed reduction products. The obtained results (data not shown) indicated that the electrolyte composition may influence the efficiency of the electrochemical processes, however, the type of the observed products was identical in all cases. The highest conversion efficiency of 1-nitroacridine molecule in the EC cell was achieved using H_2O-MeOH (1:1, *v/v*) with 0.1% FA as the electrolyte. In addition, the use of MeOH as an organic modifier resulted in the increased signal intensity of the selected mass ions because it was better than ACN in diminishing the adsorption of electrochemical products

9

on the surface of the working electrode. H_2O-MeOH electrolyte solution also produced the lowest mass background noise in positive total ion chromatograms.

The basic criterion applied for choosing the best electrode material to be used in further electrochemical simulations were the signals obtained in two-dimensional (2D) mass voltammograms (Fig. 3). Depending on the electrode used, we found significant quantitative differences in the generation of 1-nitroacridine products. Although both GC and BDD electrodes have a wide potential window, the highest yields and better detectability of 1-nitroacridine reduction products were achieved with the BDD electrode. The special properties of the BDD electrode, such as reduced fouling compared to other electrodes, its high physical, chemical, and response stability, make it well suited for any electroanalytical studies [26].

To summarize this stage of the research, 1-nitroacridine was successfully used as a model compound for the simulation of the reductive metabolic pathway of nitroaromatics by on-line EC/MS. The electrochemical conversion of 1-nitroacridine with m/z 225 ([M+H]$^+$) included the formation of four major products (Fig. 3). As can be seen from the 2D mass voltammograms, a drop in the intensity of the signal from the parent compound ion was attributed to a growth in the intensity of signals coming from its electrochemical products. Based on the data from direct ESI-MS and off-line LC/ESI-MS analyses we proposed the putative chemical structures of the obtained products (Table 2). Meanwhile, we found that the possible products of nitro group reduction that may be nitroso with m/z 209 (parent - 16 Da) and hydroxylamine with m/z 211 (parent - 14 Da) derivatives had a tendency to be formed at a similar reduction potential range, while amine species with m/z 195 (parent - 30 Da) was mostly formed at more negative reduction potentials. These observations were in good agreement with the reported earlier electrochemical behaviour of nitroaromatics in an aqueous medium [14]. In further electrochemical simulation of the reductive metabolism of UAs, we decided to apply two potential ranges (1) -1500 - -500 mV and (2) -2500 - -1500 mV. A product with m/z 401 (parent + 176 Da) corresponding to azoxy derivative exhibited very little signal intensity, while no significant signals were observed for other dimerization products such as azo and hydrazine species. Considering that only amino product was detected after reduction of 1-nitroacridine in

10

in vitro biological systems (data not shown), EC/MS can be assumed as a convenient tool for predicting reductive metabolic processes.

3.2. Electrochemical simulation of UAs reductive metabolism

Nitroaromatic compounds are relatively rare in nature but they can be introduced into living organisms in the form of therapeutics, where often undergo redox processes [27]. Reactive metabolites, that occur as a result of reductive metabolism, may be then responsible for drug therapeutic or toxic effects on the body. Due to the wide range of metabolic possibilities, drugs with the nitroaromatic group in their structure are still an attractive part of chemotherapy. The reduction of the nitro group seems to be one of the steps leading to the formation of bioactive metabolites also in the case of UAs.

The electrochemical simulation of UAs reductive metabolism was carried out under the optimized experimental conditions determined above. At first, on-line EC/ESI-MS experiments without chromatographic separation were carried out for both compounds to obtain an overview of the possible transformation products. The 2D mass voltammograms presented at the top of the Fig. 4 are a graphical representation of the pattern of the conversion of C-2028 with *m/z* 586 ([M+H]⁺) and C-2053 with *m/z* 600 ([M+H]⁺) in the EC cell. These ion mass intensity-potential curves clearly indicated a similar trend towards the specific reduction of the nitroaromatic functional group for both studied compounds. A correlation between parent molecule signal decrease and reduction product signal increase could be observed over potential sweeping.

Both C-2028 and C-2053 showed the formation of mass ions at *m/z* of (parent - 30 Da), which may suggest amine species. During EC/MS experiments the signals at *m/z* 556 and *m/z* 570, respectively, were observed at a high reduction potential. In turn, the formation of C-2028 and C-2053 species which produced ions at *m/z* 568 and *m/z* 582 (parent - 18 Da), respectively, required a lower reduction potential. C-2028 product ion at *m/z* 572 that corresponded to the lack of 14 Da to the parent [M+H-14]⁺ was also acquired, though its signal intensity was very low. An analogous product of C-2053 has not been obtained electrochemically. Electron-donating groups, such as methyl group in C-2053 molecule at the

11

end opposite to the nitro group, produce an enhancement of the push-pull effect in the molecules. This may explain the decreased stability of this intermediate product of the nitro group transformations. After all, it should be emphasized that all the *m/z* values reported above indicate that these products still possessed the structure of bisacridine dimer. Monomeric derivatives constituted the second group of electrochemical transformation products of UAs. Three major products of C-2028 which showed intense ions at *m/z* 241, 307, 364, and three of C-2053 at *m/z* 236, 255, 364 were detected. No relevant signals were observed for dimerization products such as azoxy, azo, and hydrazine species during EC/MS experiments.

3.3.   Characterization of electrochemical products

As summarized in Table 2, six and five main products of C-2028 and C-2053, respectively, were observed by electrochemistry and detected in the ESI (+) source. However, as the signal intensity in ESI-MS strongly depends on the ionization and, thus, on the polarity of the individual compounds, no conclusions on their real concentrations could be drawn. In contrast, more detailed analysis via off-line LC/ESI-MS provided further information about the hydrophobic selectivity and the existence of possible isomers of the emerging products found in on-line EC/ESI-MS experiments (bottom of the Fig. 4).

Considering the products of C-2028 and C-2053 with retained the bisacridine dimer structure, analysis of their UV-vis spectra confirmed structural changes within 1-nitroacridine rather than imidazoacridinone chromophore. In particular, the UV-vis spectra of products at *m/z* 568 and *m/z* 582 (parent - 18 Da) differed significantly from that of the substrates. This suggested that these must be structures with a strongly changed system of double bonds which may be associated with the formation of a new chromophore system. Separation of the products by reversed-phase LC revealed that each of them occurred only in one peak indicating the presence of one isomer of each compound. We found that the peaks at *m/z* 556 and *m/z* 570 (parent - 30) had shorter retention times than that of the appropriate substrate. The peak positions suggested a less polar nature of these products compared to the parent compounds. In turn, the peaks of *m/z* 568 and *m/z* 582 products appeared after the peaks corresponding to the substrates what indicates their more polar nature than that of the

substrates. Only C-2028 product at *m/z* 572 (parent - 14), which showed quite good intensity in the EC/MS system, probably due to low stability escaped LC/ESI-MS analysis.

In the next stage, some products of C-2028 electrochemical conversion, concerned above, were fully characterized by tandem mass spectrometry. Generally, MS/MS data acquired for these products were in good correlations with predicted masses (relative mass error ≤ 4.7 ppm). Their structures were proposed taking into consideration the trends of nitro group transformation [13,14].

ESI (+) Q-TOF-MS/MS spectrum obtained for *m/z* 556 ion showed fragment ions at *m/z* 195, 248, and 347 (Fig. 5A). Whereas this former, with the highest intensity, can be assigned to 1-aminoacridine (an amino derivative of 1-nitroacridine that was mentioned above), these latter can indicate the protonated forms of imidazoacridinone monomer substituted methanimine ($-N=CH_2$) or aminopropyl-*N*-methylaminoallyl ($-NH(CH_2)_3N(CH_3)CH_2CH=CH_2$) side chain, respectively. In view of the foregoing, we can conclude that the nitro group of both investigated UAs was simply electrochemically reduced to the corresponding amine derivatives.

In ESI (+) Q-TOF-MS/MS experiment, *m/z* 568 ion produced fragment ions at *m/z* 248 and *m/z* 262 which were formed by the loss of 320 and 306 Da, respectively (Fig. 5B). In turn, an analogous *m/z* 582 product ion, which was found after electrochemical conversion of C-2053, revealed fragment ions at *m/z* 248 and *m/z* 276 (data not shown). As it was established before, *m/z* 248 ion may refer to an unchanged imidazoacridinone derivative with a small linker fragment. Therefore, its existence suggested that the electrochemical conversion of C-2028 (C-2053) had to occur on the nitroacridine moiety and/or somewhere in the linker. In addition, the outgoing fragment of 306 Da, which left the most abundant fragment ion at *m/z* 262 (*m/z* 276), most likely corresponded to an imidazoacridinone with retained aminopropyl-*N*-methyl ($-NH(CH_2)_3NH(CH_3)$) side chain. Considering that the formation of a five-membered ring structure was evidenced for a key compound of the ledakrin reduction pathway [21], we suggest here that product at *m/z* 568 (*m/z* 582) might also contain a similar ring. On the one hand, the proximity of nitrogen atoms at positions 1 and 9 of the acridine core (Fig. 2B) seems

13

to enable fast intramolecular cyclization to adopt such a final structure. Moreover, it is reported that protic acidic medium may favour protonation on the nitro group [28]. Therefore, we postulate that the product at *m/z* 568 (*m/z* 582) was formed through an intermediate product with the protonated nitro group (-NO$_2$H$^+$) (Fig. 6). However, the energy of the protonated nitro group is very low. To stabilize the resulting structure, a new covalent bond within the same molecule should be formed between the nitrogen atom from the protonated nitro group and the nitrogen atom from the secondary amine, with the simultaneous release of a water molecule. In this way, the heterocyclic *N*-oxide compound might have been obtained. Further, dehydrogenation could additionally occur in the linker to increase the delocalization of electrons and thus also the stability of a molecule by resonance.

The case of tirapazamine [29], which is an aromatic heterocyclic di-*N*-oxide, shows that *N*-oxide compounds may exhibit potent activities against various human solid tumors. In fact, *N*-oxide of antitumor drugs may act as prodrugs that are activated only at very low levels of oxygen (hypoxia) to highly reactive free radicals causing the degradation of cell biomolecules (*i. e.*, DNA, proteins). These conditions are a characteristic feature of solid tumors, which are known to be resistant to radiotherapy and to most antitumor drugs [30]. In this respect, the combination of UA molecule with conventional antitumor treatment could be particularly effective. We conclude that the uniqueness of the UA antitumor agent consists of an excellent selectivity based on the intrinsic *N*-oxide-specific mechanisms of action, while imidazoacridinone monomer may presumably be a DNA-targeting unit.

Taking into consideration strongly acidic reduction conditions, a product at *m/z* 572 was tentatively characterized as hydroxylamine derivative, the common reduction product of the majority of nitroaromatic compounds [13,14]. Unfortunately, it was difficult to obtain its ESI (+) Q-TOF-MS/MS spectrum. The same *m/z* value may be also attributed to the *N*-demethylation product on a nitrogen atom in the linker between the UA monomers. However, this electrochemical product of C-2028 was generated under oxidation conditions and, in contrast to the proposed hydroxylamine, it gave a strong peak in LC/ESI-MS analysis (data not shown).

14

Electrochemical conversion of the studied UAs also resulted in the formation of a few monomeric products. Product ion at m/z 364 was characterized by identical retention times (less polar than the substrates) both for C-2028 as well as C-2053. Comparison of its experimentally observed m/z and theoretical m/z allowed us to assume that this product may contain a chromophore system of imidazoacridinone with the whole aminopropyl-N-methylaminopropylamino (-NH(CH$_2$)$_3$N(CH$_3$)(CH$_2$)$_3$NH$_2$) linker. Moreover, the C-2028 product ion at m/z 307 and the C-2053 product ion at m/z 236 could be stable products of further degradation of the linker wherein, imidazoacridinone core remained intact (Fig. 7). Although these showed quite good intensities in the EC/MS system, in chromatographic analysis these were found in small amounts. Further investigations of the structure of product ion at m/z 364 were performed by means of ESI (+) Q-TOF-MS/MS. The mass spectrum showed fragment ions at m/z 236, 248, 276, 307, and 347 that are possibly the result of linker degradation. In turn, products at m/z 241 and m/z 255 (data not shown) likely refer to derivatives that have a 1-nitroacridinone core, whereas m/z 481 indicated the presence of a dimer of the former. We suspect that the presence of such monomeric products is due to spontaneous hydrolysis of the UA molecules that have taken place in an aqueous medium and under specific conditions of electrochemical reactions.

Presented tentative structures of the products of electrochemical conversion of C-2028 and C-2053 were also proposed based on our previous studies on P450-mediated metabolism of monomeric imidazoacridinone [20] and 1-nitroacridine [21] derivatives. These considerations were also supported by the fact that electrochemical simulation of UAs reduction showed good agreement with the biotransformation reactions with human recombinant P450 isoenzymes and/or rat liver microsomes (unpublished data). Summing up, we have shown here that the nitro group of C-2028 and C-2053 easily underwent electrochemical transformations what resulted in the formation of the products with different chemical reactivity. The one containing the N-oxide motif seems to be particularly interesting because it could generate highly reactive radicals selectively under hypoxic conditions. This may have significant potential in the field of antitumor drug development.

15

3.4. Characterization of GSH and DTT adducts

C-2028 and C-2053 were subjected to electrochemical transformations in order to simulate the formation of reactive intermediate metabolites, which are known to form adducts with small molecule trapping agents. Characterization of these adducts can provide indirect data about the structure of the reactive species they are derived from, thereby providing an understanding of potential bioactivation mechanisms [15]. In this work, reduced GSH and DTT were tested in terms of their capability to trap reactive intermediate products from electrochemical reduction of the investigated UAs.

In the case of C-2028, an ion peak related to GSH adduct was seen at *m/z* 873 [M+H]+ (parent - 18 + 305 Da) in a post-electrochemical incubation mixture containing 5 mM GSH, and it was not observed in the absence of GSH (Fig. 8A). Similarly, an ion peak detected at *m/z* 720 [M+H]+ (parent - 18 + 152 Da) was formed only when the mixture obtained from the electrochemical analysis was exposed to 5 mM DTT for 30 min incubation at 37ºC (Fig. 8B). It was assumed that this peak represented DTT adduct because it was not observed in the absence of DTT. Interestingly, we found that the appearance of both *m/z* 873 and *m/z* 720 product ions was associated with the disappearance of the C-2028 electrochemical product exhibiting an ion peak at *m/z* 568, which was described above. Hence, GSH or DTT conjugations were expected to take place exactly with this product or its derivative.

The putative GSH and DTT adducts were detected by LC/MS/MS and the adduct peaks were monitored by UV-vis spectroscopy (Table 3). MS/MS data acquired for them were in good correlations with predicted masses. The obtained fragmentation pattern for GSH adduct, measured via ESI (+) Q-TOF-MS/MS, showed a strong fragment ion at *m/z* 568 indicative of the loss of 305 Da, what signified conjugation with at least one GSH moiety. This observation was supported by the presence of a fragment ion at *m/z* 308 corresponding to the protonated GSH molecule. In turn, a small fragment ion at *m/z* 744 was consistent with the loss of anhydroglutamic acid (a neutral fragment of 129 Da) from the protonated GSH adduct. The ESI (+) Q-TOF-MS/MS of *m/z* 720 ion, which was assigned to DTT adduct, produced two fragment ions at *m/z* 568 and *m/z* 414, respectively. The first one was proposed to arise via

16

the loss of one DTT molecule as neutral species, while the second fragment ion may correspond to an adduct of GSH and product at m/z 262, which was described above as a key fragment ion of the C-2028 reduction product at m/z 568.

The presence of fragment ion at m/z 568, both in fragmentation patterns for DTT and GSH adducts, supported their proposed structures in which adduct formation appeared to be occurring on the nitroacridine rather than on the imidazoacridinone moiety. Indeed, we found that the UV-vis spectra of both adducts were significantly different from that of the substrate but resembled the UV-spectrum of the product probably containing the *N*-oxide motif, which indicated substantial changes in the environment around the nitroacridine chromophore system. Our predictions were in accordance with the assumption that GSH as well as DTT trap soft electrophiles with their thiol group. In the light of the above, the nucleophilic attack of GSH or DTT on the C-2028 molecule most likely occurred before the final reduction of the nitro group, or the reduction and nucleophilic substitution happened simultaneously. The presence of the nitro group in aromatic system could facilitate this substitution.

Contrary to C-2028, C-2053 did not show the formation of any GSH and DTT adducts, although an analogous electrochemical product at m/z 568 (parent - 18) was also observed for this compound. Thus, it is expected that the most likely conjugation site with GSH or DTT was the position *para* to the nitro group. It is occupied by a methyl substituent in the C-2053 molecule what significantly diminishes its susceptibility to interactions with trapping agents. The proposed here DTT-derived substitution of reactive intermediate has been previously described for antitumor drug ledakrin [21]. These results revealed a novel metabolic activation pathway of UAs and describe the effect of structural modification on reactive metabolite trapping/toxicity. Summing up, the predictive knowledge about the reactivity of specific intermediate reduction products of UAs should have a significant impact on the reaction of these agents with cell biomolecules, especially with DNA. This provides the background for future studies that may include the investigation of UA metabolism in tumor cells.

4. Conclusions

In the present study, we took a close look into the electrochemical simulation of reductive metabolism of the selected nitroaromatic UAs of antitumor activity. We have obtained effective electrosynthesis of hydroxylamine and amine species, which were in good agreement with the products of enzymatic reactions (*i. e.*, human recombinant P450 isoenzymes, liver microsomes). Thus, this work confirmed the usefulness of the electrochemical approach to aid the study on transformations of compounds that contain nitro moiety. Additionally, the electrochemical reduction of C-2028 and C-2053 resulted in the generation of putative *N*-oxide intermediates, which were reported herein for the first time. A systematic binding of such species with nucleophilic GSH and DTT molecules was observed in the reductive metabolism of antitumor C-2028, but not C-2053, what indicated the position *para* to the nitro group to be the most likely site of nucleophilic substitution. The above knowledge will permit the future study on the interactions of this *N*-oxide derivative with potential targets of biological significance. According to the described results, it was concluded that UAs and/or their reduction products require metabolic activation before they exhibit any cytotoxic and antitumor activities. Compounds of therapeutic importance that contain *N*-oxide motif may act as prodrugs, which are activated to highly reactive free radicals only under oxygen-depleted (hypoxic) conditions characteristic of solid tumors. Therefore, we expect that the specific reduction pathway of UAs will express a significant potential in the development of selective antitumor therapy with these drug candidates.

Author statement

conceptualization: Potęga

methodology: Potęga

validation: Potęga, Paczkowski

formal analysis: Potęga, Paczkowski, Paluszkiweicz

data analysis: Potęga, Paczkowski

writing – original draft preparation: Potęga, Mazerska

writing – review and editing: Potęga

visualization: Potęga

All authors have approved the manuscript.

Conflicts of interest

There are no conflicts to declare.

Acknowledgements

References

[1] Z. Zhang, W. Tang, Drug metabolism in drug discovery and development, Acta Pharm. Sin. B, 8 (2018) 721-732.

[2] G. N. Kumar, S. Surapaneni, Role of drug metabolism in drug discovery and development, Med. Res. Rev. 21 (2001) 397-411.

[3] T. A. Baillie, M. N. Cayen, H. Fouda, R. J. Gerson, J. D. Green, S. J. Grossman, L. J. Klunk, B. LeBlanc, D. G. Perkins, L. A. Shipley, Drug metabolites in safety testing, Toxicol. Appl. Pharmacol. 182 (2002) 188-196.

[4] F. P. Guengerich, Common and uncommon cytochrome P450 reactions related to metabolism and chemical toxicity, Chem. Res. Toxicol. 14 (2001) 611-650.

[5] E. F. Brandon, C. D. Raap, I. Meijerman, J. H. Beijnen, J. H. Schellens, An update on in vitro test methods in human hepatic drug biotransformation research: pros and cons, Toxicol. Appl. Pharmacol. 189 (2003) 233-246.

[6] A. Costa, B. Sarmento, V. Seabra, An evaluation of the latest in vitro tools for drug metabolism studies, Expert Opin. Drug Metab. Toxicol. 10 (2014) 103-119.

[7] W. Lohmann, U. Karst, Biomimetic modelling of oxidative drug metabolism: strategies, advantages and limitations, Anal. Bioanal. Chem. 391 (2008) 79-96.

[8] U. Bussy, M. Boujtita, Advances in the electrochemical simulation of oxidation reactions mediated by cytochrome P450. Chem. Res. Toxicol. 27 (2014) 1652-1668.

[9] E. Nouri-Nigjeh, R. Bischoff, A. P. Bruins, H. P. Permentier, Electrochemistry in the mimicry of oxidative drug metabolism by cytochrome P450s. Curr. Drug Metab. 12 (2011) 359-371.

[10] H. Faber, D. Melles, C. Brauckmann, C. A. Wehe, K. Wentker, U. Karst, Simulation of the oxidative metabolism of diclofenac by electrochemistry/(liquid chromatography/)mass spectrometry, Anal. Bioanal. Chem. 403 (2012) 345-354.

[11] A. Baumann, W. Lohmann, B. Schubert, H. Oberacher, U. Karst, Metabolic studies of tetrazepam based on electrochemical simulation in comparison to *in vivo* and *in vitro* methods, J. Chromatogr. A 1216 (2009) 3192-3198.

[12] S. Jahn, A. Baumann, J. Roscher, K. Hense, R. Zazzeroni, U. Karst, Investigation of the biotransformation pathway of verapamil using electrochemistry/liquid chromatography/mass spectrometry – A comparative study with liver cell microsomes, J. Chromatogr. A1218 (2011) 9210-9220.

[13] J. A. Squella, S. Bollo, L. J. Nunez-Vergara, Recent developments in the electrochemistry of some nitro compounds of biological significance, Curr. Org. Chem. 9 (2005) 565-581.

[14] U. Bussy, Y.-W. Chung-Davidson, K. Li, W. Li, Phase I and phase II reductive metabolism simulation of nitro aromatic xenobiotics with electrochemistry coupled with high resolution mass spectrometry, Anal. Bioanal. Chem. 406 (2014) 7253-7260.

20

[15] A. C. Macherey, P. M. Dansette, Biotransformations leading to toxic metabolites: chemical aspects, in: The Practice of Medicinal Chemistry (Fourth Ed.), Academic Press, Cambridge, 2015, pp. 585-614.

[16] M. P. Grillo, Detecting reactive drug metabolites for reducing the potential for drug toxicity, Expert Opin. Drug Metab. Toxicol. 11 (2015) 1281-1302.

[17] J. K. Konopa, B. Horowska, E. M. Paluszkiewicz, B. Borowa-Mazgaj, E. A. Augustin, A. Skwarska, Z. Mazerska, Asymmetric bis-acridines with antitumour activity and use thereof, European Patent No.: EP 3 070 078 A1, 2017-10-04.

[18] J. K. Konopa, B. Horowska, E. M. Paluszkiewicz, B. Borowa-Mazgaj, E. A. Augustin, A. Skwarska, Z. Mazerska, Asymmetric bis-acridines with antitumour activity and their uses, US Patent No.: US10202349B2, 2019-02-12.

[19] W. M. Cholody, S. Martelli, J. Paradziej-Lukowicz, J. Konopa, 5-[(Aminoalkyl)amino]imidazo[4,5,1-de]acridin-6-ones as a novel class of antineoplastic agents. Synthesis and biological activity, J. Med. Chem. 33 (1990a) 49-52.

[20] A. Wiśniewska, A. Chrapkowska, A. Kot-Wasik, J. Konopa, Z. Mazerska, Metabolic transformations of antitumor imidazoacridinone, C-1311, with microsomal fractions of rat and human liver, Acta Biochim. Pol. 54 (2007) 831-838.

[21] K. Gorlewska, Z. Mazerska, P. Sowiński, J. Konopa, Products of metabolic activation of the antitumor drug Ledakrin (Nitracrine) *in vitro*, Chem. Res. Toxicol. 14 (2001) 1-10.

[22] R. M. Acheson, Acridines, in: R. M. Acheson (Ed.), The chemistry of heterocyclic compounds, Interscience Publishers, Inc., New York, 1973, pp. 71-72.

[23] A. Potęga, D. Garwolińska, A. M. Nowicka, M. Fau, A. Kot-Wasik, Z. Mazerska, Phase I and phase II metabolism simulation of antitumor-active 2-hydroxyacridinone with electrochemistry coupled on-line with mass spectrometry, Xenobiotica 49 (2019) 922-934.

[24] A. Potęga, D. Żelaszczyk, Z. Mazerska, Electrochemical simulation of metabolism for antitumor-active imidazoacridinone C-1311 and *in silico* prediction of drug metabolic reactions, J. Pharm. Biomed. Anal. 169 (2019) 269-278.

[25] C. Karakus, P. Zuman, Polarographic and electrochemical studies of some aromatic and heterocyclic nitro compounds Part 9. Substitutent effects on protonation of the radical ArNO2H· and its reactions with hydroxylamino and nitroso compounds in buffered mixtures of water and DMF, J. Electroanal. Chem. 396 (1995) 499-505.

[26] J. V. Macpherson, A practical guide to using boron doped diamond in electrochemical research, Phys. Chem. Chem. Phys. 17 (2015) 2935–2949.

[27] D. Olender, J. Żwawiak, L. Zaprutko, Multidirectional efficacy of biologically active nitro compounds included in medicines, Pharmaceuticals 11 (2018) 1-29.

[28] O. Exnera, S. Böhm, Protonated nitro group: structure, energy and conjugation, Org. Biomol. Chem. 3 (2005) 1838-1843.

[29] A. M. Mfuh, O. V. Larionov, Heterocyclic N-oxides – an emerging class of therapeutic agents, Curr. Med. Chem. 22 (2015) 2819-2857.

[30] J. M. Brown, Tumor hypoxia in cancer therapy, Methods Enzymol. 435 (2007) 297-321.

Figure captions

Figure 1_revised
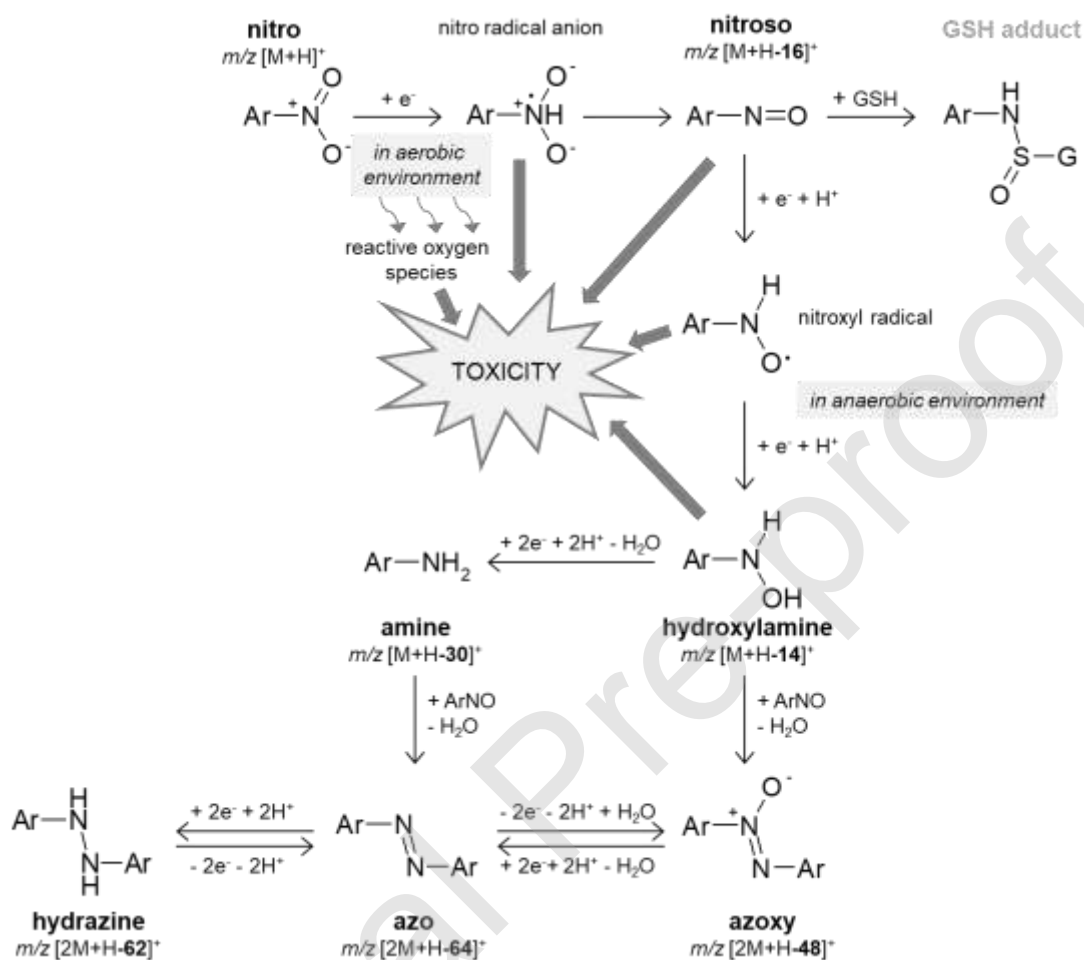
Figure 1

The general pathway of the reductive transformation of the nitroaromatic compound to corresponding nitroso, hydroxylamine, and amine species and their dimers or GSH adduct (scheme based on [14]). The theoretical positive ion masses of the products of nitro group reduction are indicated; M – a molecular mass of the parent compound.

23
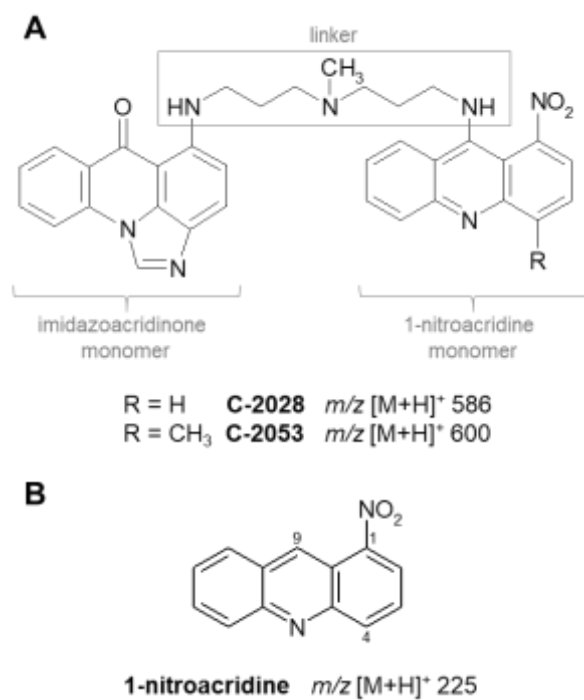
Figure 2_revised

Figure 2

Chemical structures of the investigated compounds: (A) nitroaromatic unsymmetrical bisacridines: C-2028 and C-2053; (B) 1-nitroacridine (a model compound).

24

Figure 3_revised
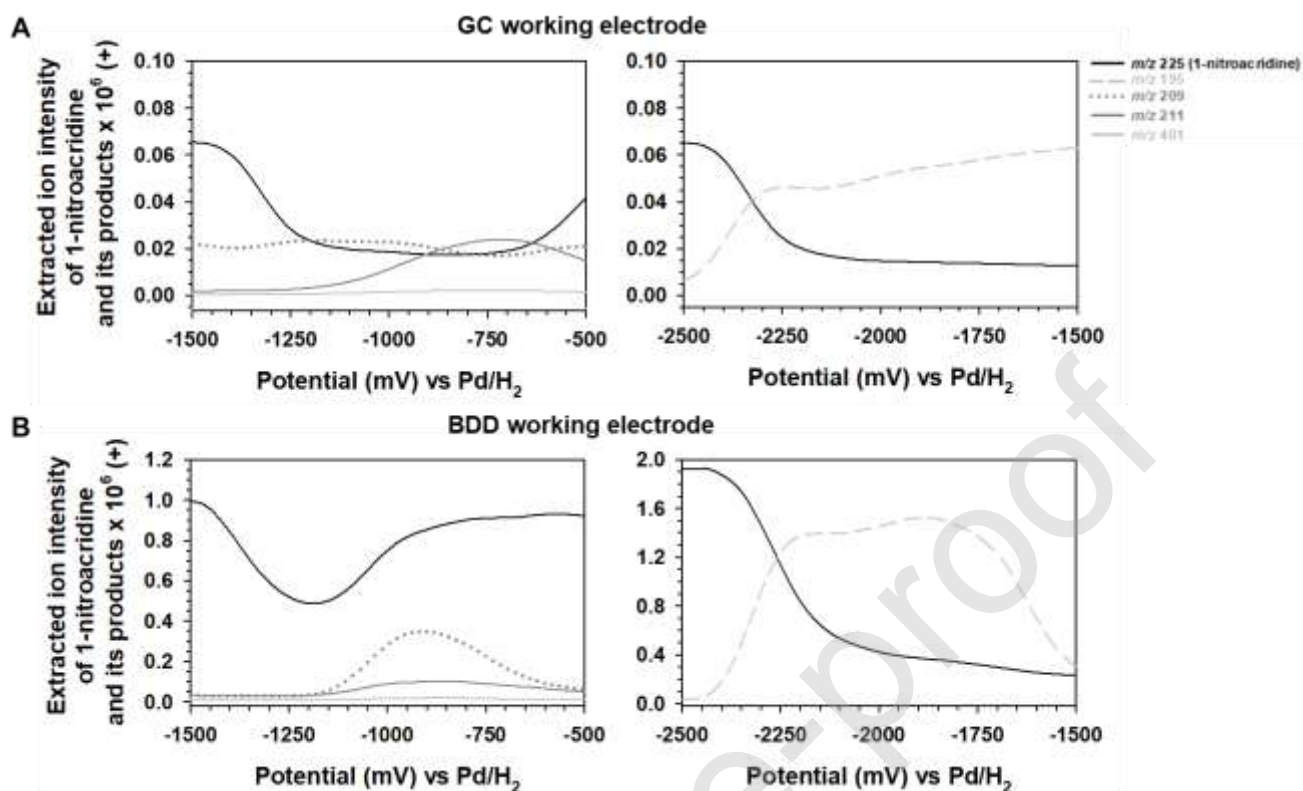
Figure 3

Impact of the type of working electrode on the electrochemical conversion of 10 μM 1-nitroacridine. Representative 2D mass voltammograms for (A) GC and (B) BDD electrode. The *m/z* ratios shown correspond to the protonated [M+H]+ (positive ion mode) 1-nitroacridine molecule and its electrochemical products (see legend). The *m/z* ratios shown have been rounded to the nearest integer. Experimental conditions: electrolyte H_2O-MeOH (1:1, *v/v*) with 0.1% FA; flow rate of electrolyte 20 μL min⁻¹; potential ranges -1500 – -500 mV and -2500 – -1500 mV; scan rate 5 mV s⁻¹; T = 21°C. All potentials were measured versus the Pd/H_2 reference electrode.

25

Figure 4_revised

Figure 4

Representative 2D mass voltammograms (at the top) and liquid chromatograms (at the bottom) resulting from the electrochemical conversion of 10 µM (A) C-2028 and (B) C-2053 at a BDD working electrode. The *m/z* ratios shown correspond to the protonated [M+H]⁺ (positive ion mode) parent compounds and their electrochemical products (see legend). The *m/z* ratios shown have been rounded to the nearest integer. Experimental conditions: electrolyte H_2O-MeOH (1:1, *v/v*) with 0.1% FA; flow rate of electrolyte 20 µL min⁻¹; potential range -1500 – -

26

500 mV; scan rate 5 mV s⁻¹; T = 21°C. All potentials were measured versus the Pd/H₂ reference electrode.

Figure 5
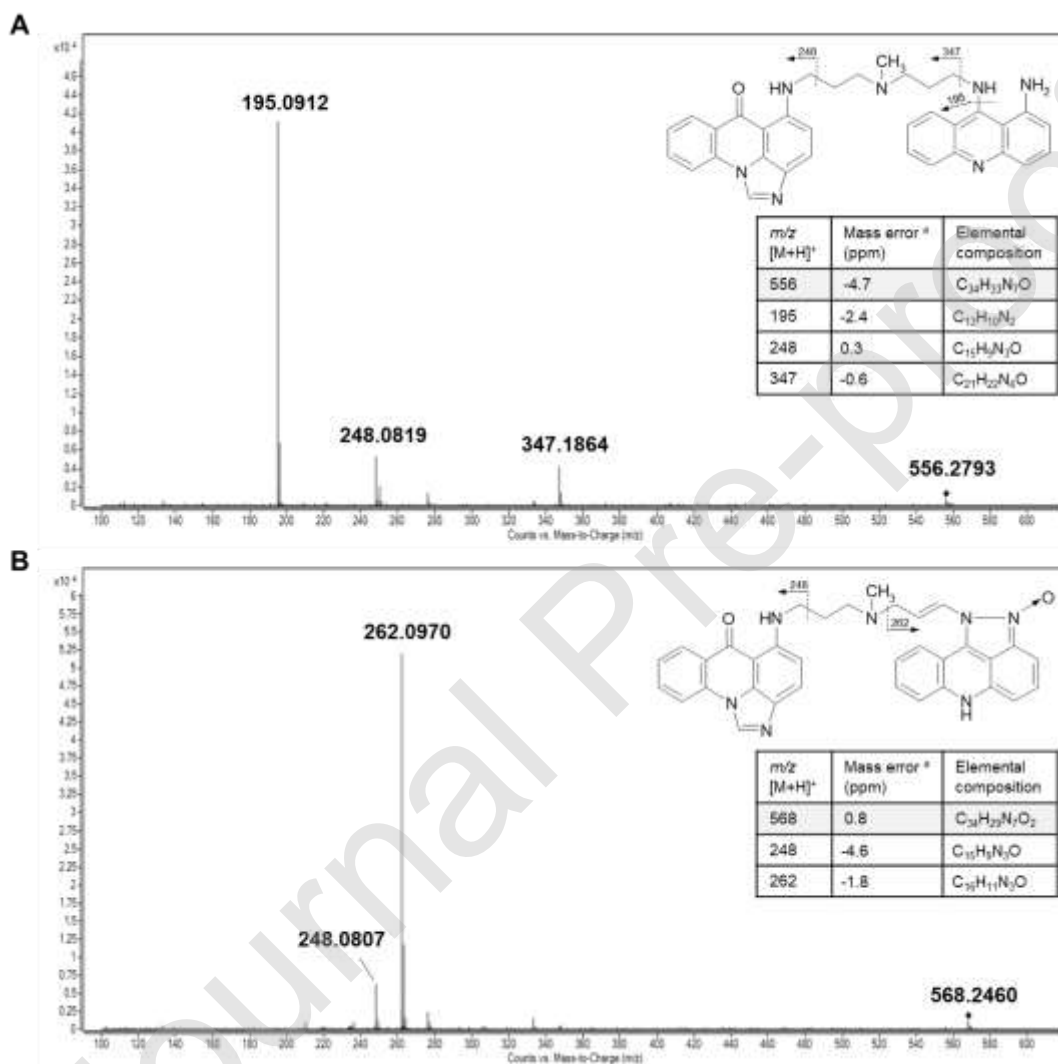
Figure 5

Representative MS/MS spectra and fragmentation patterns for (A) *m/z* 556 and (B) *m/z* 568 attributed to the products of electrochemical conversion of C-2028 molecule. *ᵃ* Exact masses were calculated using Molecular Mass Calculator freeware version v2.02.

27
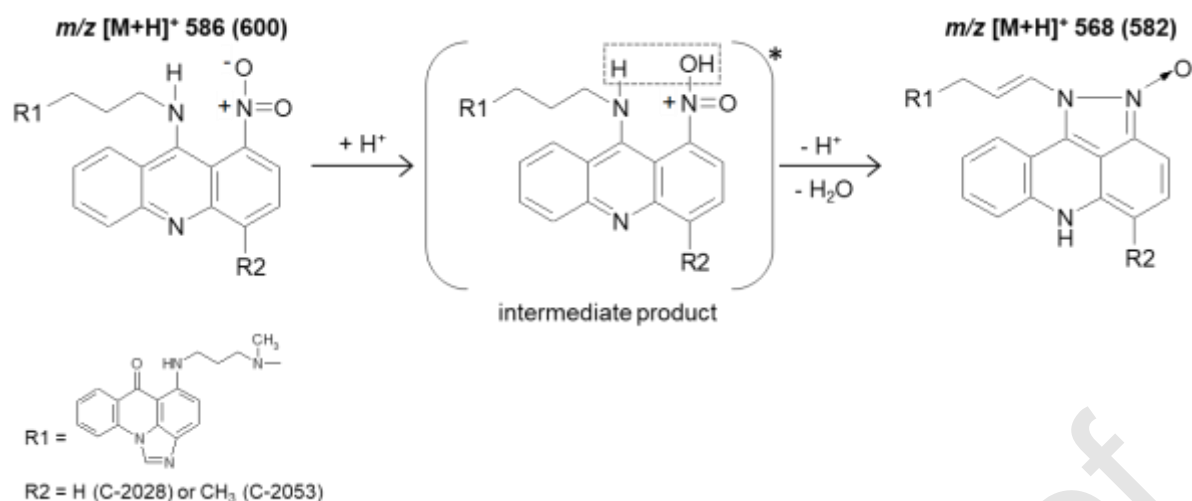
Figure 6

Figure 6

Proposed mechanism for the formation of the ions at *m/z* 568 and *m/z* 582.

Figure 7

Figure 7

Proposed degradation profile for product ion at *m/z* 364 obtained after the electrochemical conversion of C-2028 and C-2053 molecules. The *m/z* ratios shown have been rounded to the nearest integer.

28
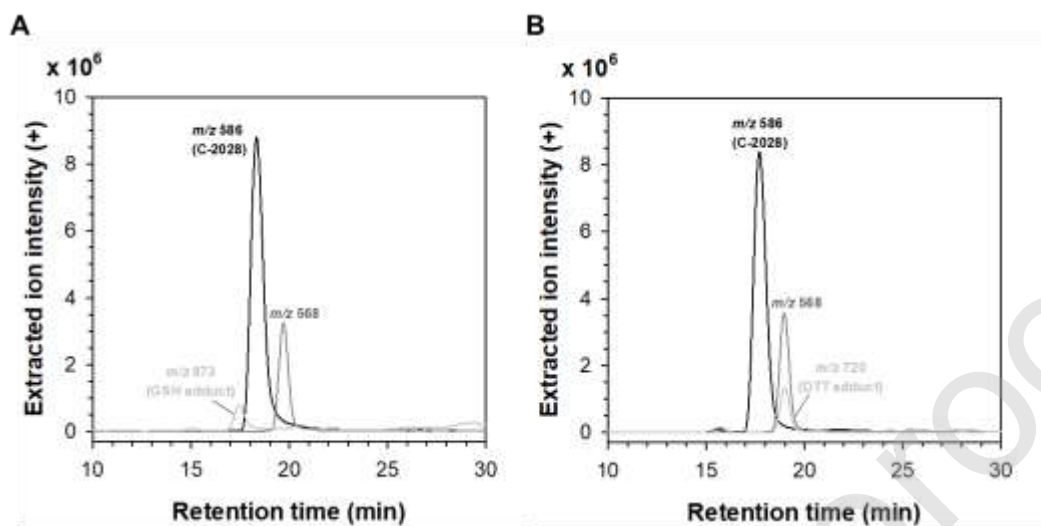
Figure 8

Figure 8

Representative chromatograms (positive ion mode) of (A) *m/z* 873 and (B) *m/z* 720 attributed to GSH and DTT adducts, respectively, obtained after the electrochemical conversion of the C-2028 molecule. Product ion at *m/z* 568 was observed only in the absence of GSH or DTT. The *m/z* ratios shown have been rounded to the nearest integer.

Table 1
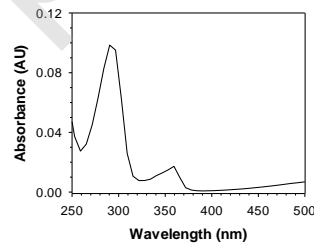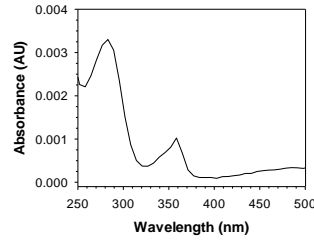
Mass spectrometry parameters applied in direct EC/ESI-MS, LC/ESI-MS, and LC/Q-TOF-MS/MS experiments for the determination of accurate masses of product ions and getting ion fragmentation patterns.

Parameter	Value or setting
Ion source type	Dual ESI
Ion polarity	Positive
The range of *m/z*	100 – 1500
MS operating mode	Scan
Rate	1.5 spectra s^{-1}
Nebulizing gas (N$_2$) pressure	35 psi
Nebulizing gas flow	1.5 L min^{-1}
Drying gas (N$_2$) flow	10 L min^{-1}
Drying gas temperature	350°C
Fragmentor	175 V
Skimmer	45 V
OCT 1 RF Vpp	750 V
Capillary voltage	3500 V
MS/MS method	Targeted
- Slope	- 4 *m/z*
- Offset	- 5 V
- Collision energy	- 30 eV

30
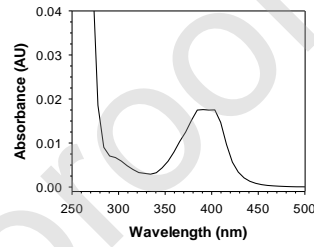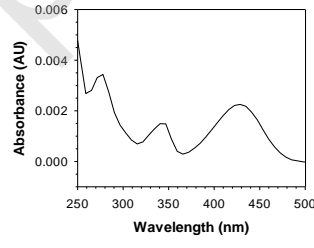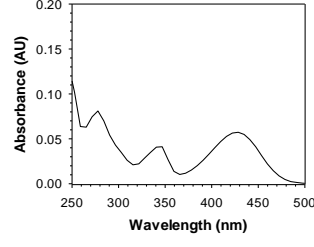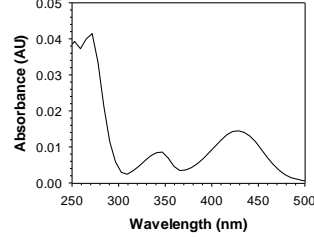
Table 2
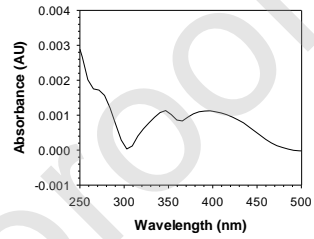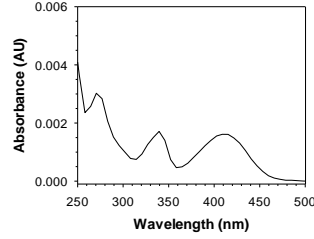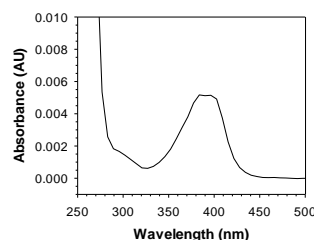
Summary of the products of 1-nitroacridine, C-2028, and C-2053 compounds generated in the electrochemical cell and detected by on-line ESI-MS and/or by off-line LC/ESI-MS. The m/z ratios shown have been rounded to the nearest integer.

Compound	Electrosynthesis product / Elemental composition	m/z [M+H]$^+$	Retention time (min)	UV-vis spectrum	Proposed by	Formation by P450 and/or rat liver microsomes
1-nitroacridine $C_{13}H_8N_2O_2$ m/z [M+H]$^+$ = 225	amine / $C_{13}H_{10}N_2$	195	11.65		on-line EC/ESI-MS off-line EC LC/ESI-MS	+
	nitroso / $C_{13}H_8N_2O$	209	15.41 [a]	ND [b]	on-line EC/ESI-MS	-
	hydroxylamine / $C_{13}H_{10}N_2O$	211	10.55		on-line EC/ESI-MS off-line EC LC/ESI-MS	-
	azoxy / $C_{26}H_{16}N_4O$	401	ND [b]	ND [b]	on-line EC/ESI-MS	-

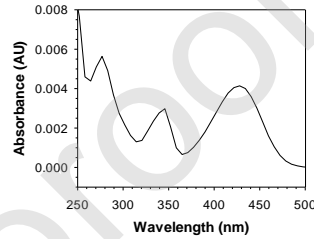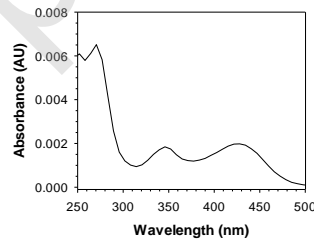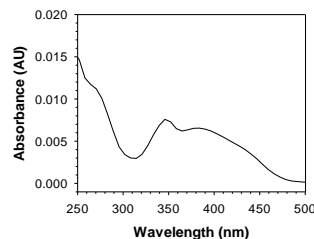31

C-2028 $C_{34}H_{31}N_7O_3$ *m/z* $[M+H]^+ =$ 586	1-nitroacridinone / $C_{13}H_8N_2O_3$	241	24.02		on-line EC/ESI-MS off-line EC LC/ESI-MS	-
	$C_{18}H_{18}N_4O$	307	17.18 [a]		on-line EC/ESI-MS off-line EC LC/ESI-MS	+
	$C_{21}H_{25}N_5O$	364	14.26		on-line EC/ESI-MS off-line EC LC/ESI-MS	+
	amine / $C_{34}H_{33}N_7O$	556	16.95		on-line EC/ESI-MS off-line EC LC/ESI-MS	+

	$C_{34}H_{29}N_7O_2$	568	19.94		on-line EC/ESI-MS off-line EC LC/ESI-MS	+
	hydroxylamine / $C_{34}H_{33}N_7O_2$	572	ND [b]	ND [b]	on-line EC/ESI-MS	-
C-2053 $C_{35}H_{33}N_7O_3$ *m/z* [M+H]$^+$ = 600	$C_{14}H_9N_3O$	236	24.19 [a]		on-line EC/ESI-MS off-line EC LC/ESI-MS	-
	4-methyl-1-nitroacridinone / $C_{14}H_{10}N_2O_3$	255	25.13 [a]		on-line EC/ESI-MS off-line EC LC/ESI-MS	-

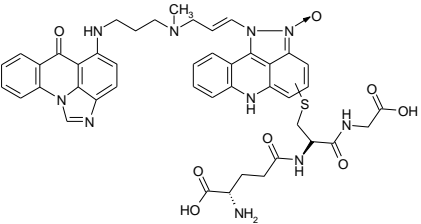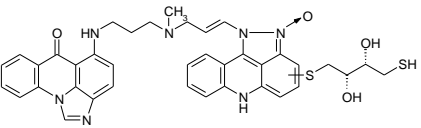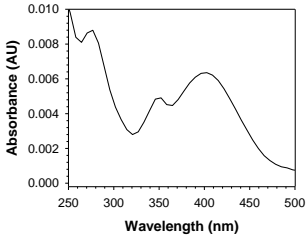| Formula	m/z	RT	UV-Vis spectrum	Method	Ion
$C_{21}H_{25}N_5O$	364	14.26		on-line EC/ESI-MS off-line EC LC/ESI-MS	-
amine / $C_{35}H_{35}N_7O$	570	17.24		on-line EC/ESI-MS off-line EC LC/ESI-MS	+
$C_{35}H_{31}N_7O_2$	582	21.57		on-line EC/ESI-MS off-line EC LC/ESI-MS	+
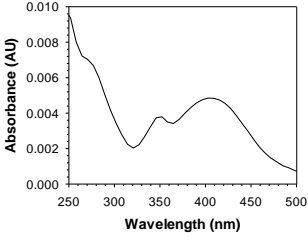
[a] Trace, trace amounts observed.
[b] ND, not detected.

Table 3

Overview of *m/z* and fragmentations for ions attributed to the respective GSH and DTT adducts of C-2028.

The proposed structure	Representative measured *m/z* [M+H]+	Molecular formula	Relative mass error [a] (ppm)	Key MS/MS fragment ions	Retention time (min)	UV-vis spectrum
GSH adduct	873.3116	$C_{44}H_{44}N_{10}O_8S$	2.4	744, 568, 308	17.60	
DTT adduct	720.2416	$C_{38}H_{37}N_7O_4S_2$	0.7	568, 414	18.97	

[a] Exact masses were calculated using Molecular Mass Calculator freeware version v2.02.

35